Extended Defects in Graphene and Their Contribution to the Excess Specific Heat at High Temperatures

M. V. Kondrin,[1,*] Y. B. Lebed,[2] and V. V. Brazhkin[1]
[1]*Institute for High Pressure Physics RAS, 108840 Troitsk, Moscow, Russia*
[2]*Institute for Nuclear Research RAS, 117312 Moscow, Russia*

(Received 2 November 2020; accepted 2 April 2021; published 23 April 2021)

The recent experiments on fast (microsecond) pulse heating of graphite suggest the existence of sharp maximum (6500 K at 1–2 GPa) on its melting curve. To check the validity of these findings, we propose to investigate the accumulation of extended in-plane defects in graphene. Such defects would contribute to thermodynamic properties of graphene and impose the upper limit on its melting temperature. We propose a type of extended defect of graphene, consisting of pentagonal and heptagonal rings with record low formation energy, whose accumulation leads to the loss of shear rigidity of graphene at temperatures above 6400 K, thus setting the upper limit on its melting temperature. We found that this model satisfactorily explains the increase of specific heat observed in the premelting region of graphite in slow (millisecond) pulse heating experiments. However, in fast (microsecond) pulse heating experiments such an increase of specific heat was not observed, which is a strong indication of overheating that takes place in these experiments.

DOI: 10.1103/PhysRevLett.126.165501

The investigation of the thermodynamic properties of carbon near its melting curve is a challenging task from both theoretical and experimental points of view. This is especially true for the low-pressure carbon polymorph—graphite. Because of the extreme strength of interatomic bonds, the decomposition of crystal lattice of graphene takes place at very high temperatures. This situation gets more difficult at a low-pressure region due to the complexity of the graphite phase diagram near the triple point, solid-liquid vapor, at 0.01 GPa and 4800 K [1–4]. At ambient pressure graphite sublimation starts at temperatures above 4000 K, but at pressures above the triple point, its melting behavior is not that clear. Previous experimental findings of Bundy [5,6] and Togaya [7] reveal that the melting curve is smooth with a slightly pronounced maximum at 5200 K and 5 GPa. However, recent experiments [8] seem to overthrow this picture and suggest a steep maximum peaked at 6500 K and 2–5 GPa (see Fig. 1). It should be noted, that the maximum on the melting curve (especially a steep one) may point at liquid-liquid transition in the substance [9]. In graphite it could be connected with transition from a two-coordinated vapor to more dense three-four coordinated fluid at higher pressures near the diamond-fluid-graphite triple point [10–15].

This contradiction might indicate a certain flaw in execution and interpretation of the experiments. Both series of experiments use the pulse heating method for investigation of melting curve. Still, there is a significant difference between high-pressure experiments of Bundy [5,6] and Togaya [7], using millisecond pulses, and the low pressure ones (Kondratyev and Rakhel [8]) with microsecond pulses applied. This might lead to overheating of the samples at low-pressure experiments. However, low-pressure experiments of Kondratyev and Rakhel involving their interferometry technique, demonstrated almost a twofold increase of specific volume of the graphite sample

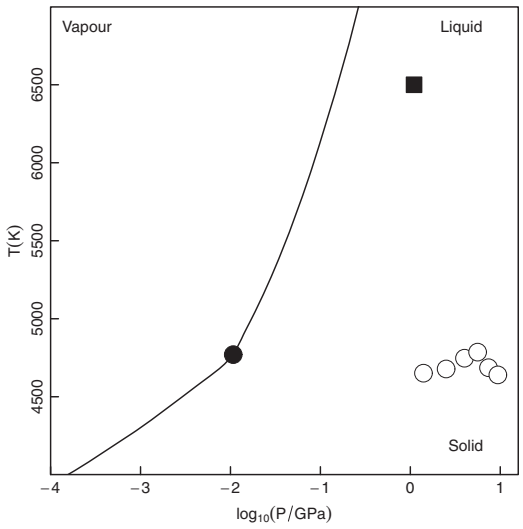

FIG. 1. Phase diagram of graphite in a low-pressure region. Solid lines designate the vapor phase boundary according to Leider *et al.* [16]. (Black filled circle) triple point vapor-solid-liquid, which corresponds to experimental results obtained by Savvatimskiy *et al.* [1].(White filled circle) melting points of graphite obtained by Togaya [7]. (Black filled square) melting point of graphite, registered in experiments of Kondratyev and Rakhel [8].

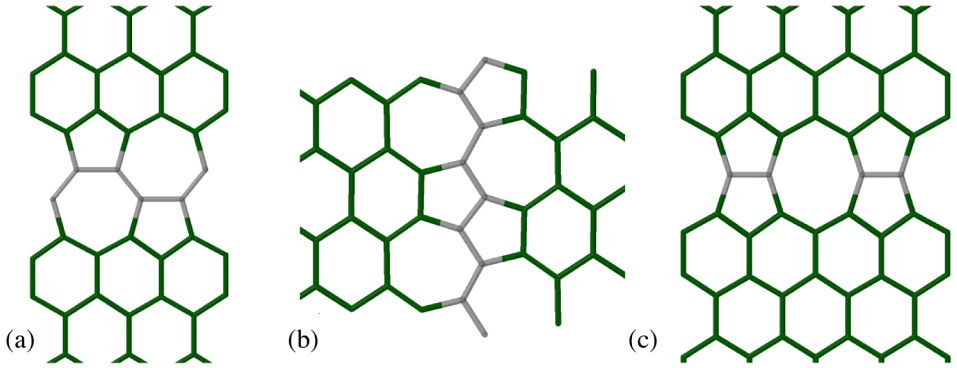

FIG. 2. Zigzag (a) and armchair (b) extended defects in graphene considered in the Letter. In (c) the artificially created extended defect in graphene [20] is shown. Solid green color depicts domains of pristine graphene. The translucent gray color marks interfacial carbon layers.

during melting. If this drastic increase of the specific volume of graphite takes place indeed, it can result as well in a significant increase of local pressure in high-pressure experiments of Bundy and Togaya. Thus, experimental points obtained by Togaya [7] at a low pressure (below 5 GPa), in fact should be attributed to higher pressures. In other words, his experiments might "overshoot" the steep maximum observed by Kondratyev and Rakhel [8] and collect data at a downward slope of the melting curve. It should be noted that results of similar to [1] low-pressure experiments with longer (millisecond) pulses, accompanied by the destruction of the measurement cell (and thus low pressure attained), produce the value $T_m = 4800$ K, which is close to the solid-liquid-vapor triple point [16].

To clarify this contradiction, *ab initio* molecular dynamic simulation would be the most valuable method. However, due to the mentioned complexity of the carbon phase diagram, this calculation is not available right now. Instead, as a provisional measure, we propose our own method [17] of *ab initio* calculation of the upper limit on the melting temperature of a substance.

Namely, we have demonstrated that the accumulation of certain types of extended defects and stacking faults can lead to the loss of shear rigidity of the sample. In some regard, this process is similar to melting, except that it proceeds without first order phase transitions. These considerations were previously used for the determination of the upper limit on the melting temperature of diamond [17]; the results obtained turned out to be very close to the real melting temperature, as found by shock wave experiments in the moderate pressure limit [18]. In this method, we propose the type of extended (planar in the case of diamond) defects and stacking faults, with the low enough formation energy and nonzero displacement vector. Both conditions allow for the relaxation of shear stress at high temperatures (above the formation energy of the defect). For diamond, various types of defect structures contributing to amorphous and liquid state were extensively studied [19], and the group of structures with the lowest formation energies (besides the diamond-lonsdaleite one) was outlined. These structures turned out to be various combinations of 5- and 7-membered cycles, embedded into diamond-lonsdaleite structure. For graphite, similar research was not accomplished, but we can act by analogy and consider various extended in-plane defects in graphene formed by pentagons and heptagons.

Two types of extended in-plane defects in graphene, formed along "zigzag" and "armchair" edges of graphene layers are shown in Figs. 2(a) and 2(b), respectively. Further, we will call these stacking faults zigzag and armchair, respectively. For comparison, we will also consider an extended defect, consisting of pentagons and octagons, which was previously artificially created in a single graphene layer, epitaxially grown on Ni substrate [20] [Fig. 2(c)]. It should be noted, however, that while zigzag and armchair stacking faults are made of a single monoatomical carbon layer (somewhat crumpled), in the last structure the interface layer contains divacancies (as it was demonstrated in Ref. [21]). This results in a different number of defect atoms in the unit cell. The zigzag structure contains four defect atoms per unit cell in one interfacial layer, armchair—eight in two layers, and pentagon-octagon one—only two in one defect layer. It should be noted that defects consisting of heptagonal and pentagonal rings were considered before (especially for isolated defects like the well-known Stone-Wales one) but in regard to extended defects the information is scarce. Although the combination of pentagons and heptagons was considered as grain boundaries in graphene [22], the first-principle calculation of their formation energies was not carried out. Detailed structural information of defect structures investigated is provided in Supplemental Material [23].

The extended graphene defects were modeled in approximately 48-atom supercell. For calculation of their formation energies, the QUANTUMESPRESSO software package was used [24]. For the density functional calculation, we employed the

Perdew-Burke-Ernzerhof exchange correlation method with norm-conserving pseudopotentials with the energy cutoff 70 Ry. For integration over the Brillouin zone, the unshifted $4 \times 1 \times 1$ Monkhorst-Pack grid was used. Crystal lattices and atom positions at a fixed external pressure were fully optimized with the dimension normal to the carbon layer being kept fixed at 10 Å until the residual force on every atom did not exceed 0.001 Ry/bohr and additional stress—0.5 kbar. The formation energy of the defect was calculated by taking the energy difference between defected structure (E) and defect-free graphene lattice (E_{host}) of similar dimensions:

$$\Delta E = E - E_{\mathrm{host}} n/n_{\mathrm{host}},$$

where n and n_{host} are the number of carbon atoms in defected and pristine graphene layers. It should be noted, however, that for an extended defect, not thus defined formation energy, but rather its normalized value (by the interface layer length or the number of atoms comprising the defect) has physical sense. We will call it a specific formation energy.

In the course of calculation, we also found that there is an appreciable displacement vector along the corresponding stacking faults, equal to 1.2 Å and to 1.0 Å for zigzag and armchair defects, respectively. According to our model, formation energy of a stacking fault is the barrier energy, which should be overcome to produce the shift of adjacent graphene layers, which is due to the random shear stress.

Specific formation energies of the considered defects differ significantly, but still they are much less than the formation energy of isolated defects in graphene. Specific formation energies per defect atom or per defect length are 0.581 eV/atom (0.475 eV/Å), 0.889 eV/atom (0.808 eV/Å), and 1.248 eV/atom (0.508 eV/Å) for zigzag, armchair, and pentagonal-octagonal defects, respectively. The last value corresponds nicely to specific formation energy reported in Ref. [21]. On the other hand, for the single vacancy defect the similar calculations yield a formation energy equal to 8.15 eV, and for the topological Stone-Wales defect [25]—4.9 eV (that is, 2.45 eV per one of two atoms constituting the defect). It is clear that the zigzag defect is the most energetically favorable one (either per unit length or per defect atom) and its formation energy is comparable to thermal fluctuation energy at the melting temperature of graphene. We should also note that this defect resembles the proposed earlier crystal structure named ψ graphene [26,27], which has extremely low additional energy in comparison to pure graphene. So, for further discussion we will consider only this defect.

The accumulation of extended defects in solid graphene at high temperature will produce an additional channel of thermodynamic relaxation and thus lead to excess specific heat above the standard Dulong-Petit "3R" value. In fact, this excess specific heat was observed in experiment on graphite [1]. As shown in Fig. 3, this additional specific heat in the premelting temperature region corresponds well to the specific heat of zigzag extended defects in graphene, calculated in our model. In this model the system is regarded as a "gaseous mixture" of two types of extended defects (which can be labeled as "shifted" or "unshifted"), separated by stacking faults. Free energy F of such a system can be calculated as

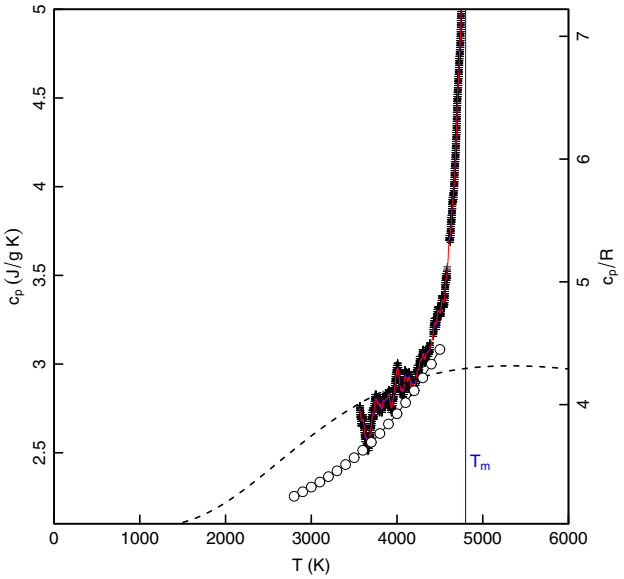

FIG. 3. Comparison (not a fit) of experimental excess specific heat with theoretical dependence obtained for extended zigzag defects with specific formation energy 0.57 eV/atom. Experimental data of graphite specific heat were obtained in the millisecond pulse heating experiment of Savvatimskiy *et al.* [1] (Plus symbol) and Sheindlin and Senchenko [28] (White filled circle). Dashed line—theoretical curve of specific heat calculated according to Eq. (1) with the Dulong-Petit "3R" additive term (the Debye temperature of graphite is ≈400 K).

$$F(T,x) = F_0(T) + 2\Delta E x + k_B T[x\ln(x) + (1-x)\ln(1-x)].$$

Here, ΔE is formation energy per atom of the interface layer (which was calculated before), and coefficient 2 catches the fact that the two stacking faults are necessary for formation of one extended defect. x is the concentration of extended defects. The minimization of free energy with respect to defect concentration allows one to estimate the equilibrium concentration of defects x and correspondingly their additional specific heat Δc_V:

$$x = \left[\exp\left(\frac{2\Delta E}{k_B T}\right) + 1\right]^{-1},$$
$$\Delta c_V = 2E\frac{dx}{dT} = \frac{\Delta E^2}{k_B T^2 \cosh^2\left(\frac{\Delta E}{k_B T}\right)}. \quad (1)$$

In the above consideration only one group of defects, oriented along one crystallographic direction, was taken

into account. There are three equivalent in-plane crystallographic directions in graphene, so the total excess specific heat should include a configurational multiplier, equal to 3. All of these notions were used while drawing the theoretical curve in Fig. 3. It is found that it closely resembles experimental data. The sharp rise of the experimental specific heat in the vicinity of the melting temperature observed in experiments was ascribed to the influence of nonequilibrium defects [1,2] but it can be due as well to the nonuniformity of the heating during pulse heating experiments, so some regions of the sample melts "earlier" (and so contribute to the divergence of the specific heat) than the average temperature registered on the surface of the sample.

Beside calculation of thermodynamic parameters in the premelting region of graphene, it is worthwhile to consider the upper limit on the melting temperature of graphene which it imposes ($\Delta E/k_B \approx 6400$ K). This is the temperature, where the accumulation of only one type of extended defect leads to the loss of shear rigidity. Although it is significantly greater than the true melting point of graphite in the triple point, we cannot rule out the possibility that this discrepancy between the real melting temperature and the estimate of its upper limit diminishes with the rise of pressure. So, this does not rule out the possibility of the existence of a large peak at the melting curve of graphite at elevated pressures, reported in Ref. [8]. However, this calculation also gives an opportunity to disprove the possibility of overheating, which could be observed in microsecond experiments of Kondratyev and Rakhel [8]. This opportunity is linked with the measurement of specific heat in the premelting region. Since extended defects contributing to excess heat are the equilibrium ones, the overheating would prevent their formation. So, the excess specific heat in that case would not be observed. Moreover, taking into account the values of melting temperature, reported in experiments, and the temperature at the maximum of excess specific heat [Eq. (1)] in equilibrium conditions, a wide but well pronounced maximum of specific heat at high pressures should be observed. The observation of such a peak would eliminate all doubts regarding possible overheating of the sample. However, in the Letter of Kondratyev and Rakhel [8], it was reported that the specific heat of graphite in the premelting region did not differ much from the Dulong-Petit law ($c_v = 3.3 \pm 0.3$ R). It means that the extended defects, which were earlier found to produce excess specific heat in much longer experiments [1,28], had no time to form in the microsecond experiments. So this is a strong indication that indeed the overheating in microseconds graphite melting experiments was achieved.

To conclude, we propose the new type of extended defect in graphene, consisting of pentagonal and heptagonal rings, with remarkably low formation energy per interface atom. Accumulation of these defects at high temperatures would significantly contribute to thermodynamic properties of graphene and eventually (at temperatures above 6400 K) leads to the loss of its shear rigidity. This process imposes an upper limit on the possible melting temperature of graphene. This model nicely explains the observation of excess specific heat, found in the premelting region at"slow" (millisecond) pulse heating experiments on graphite. Although the calculated upper limit does not immediately rule out the possibility of higher graphite melting temperature at higher pressures (observed at "fast"-microsecond experiments), but the absence of the characteristic increase of specific heat at the premelting region makes one to believe that overheating of graphite took place in these experiments.

This work is supported by the Russian Science Foundation (Grant No. 19-12-00111).

*mkondrin@hppi.troitsk.ru

[1] A. Savvatimskiy, S. Onufriev, and A. Kondratyev, Carbon **98**, 534 (2016).
[2] A. I. Savvatimskii and S. V. Onufriev, Phys. Usp. **63**, 1015 (2020).
[3] V. S. Dozhdikov, A. Y. Basharin, P. R. Levashov, and D. V. Minakov, J. Chem. Phys. **147**, 214302 (2017).
[4] C. Hull, S. Raj, and R. Saykally, Chem. Phys. Lett. **749**, 137341 (2020).
[5] F. P. Bundy, J. Chem. Phys. **38**, 618 (1963).
[6] F. Bundy, W. Bassett, M. Weathers, R. Hemley, H. Mao, and A. Goncharov, Carbon **34**, 141 (1996).
[7] M. Togaya, Phys. Rev. Lett. **79**, 2474 (1997).
[8] A. M. Kondratyev and A. D. Rakhel, Phys. Rev. Lett. **122**, 175702 (2019).
[9] V. V. Brazhkin, S. V. Popova, and R. N. Voloshin, High Press. Res. **15**, 267 (1997).
[10] G. Galli, R. M. Martin, R. Car, and M. Parrinello, Phys. Rev. Lett. **63**, 988 (1989).
[11] G. Galli, R. M. Martin, R. Car, and M. Parrinello, Phys. Rev. B **42**, 7470 (1990).
[12] J. R. Morris, C. Z. Wang, and K. M. Ho, Phys. Rev. B **52**, 4138 (1995).
[13] L. M. Ghiringhelli, J. H. Los, E. J. Meijer, A. Fasolino, and D. Frenkel, Phys. Rev. Lett. **94**, 145701 (2005).
[14] Y. D. Fomin and V. Brazhkin, Carbon **157**, 767 (2020).
[15] J. N. Glosli and F. H. Ree, Phys. Rev. Lett. **82**, 4659 (1999).
[16] H. Leider, O. Krikorian, and D. Young, Carbon **11**, 555 (1973).
[17] M. Kondrin, Y. Lebed, and V. Brazhkin, Diamond Relat. Mater. **110**, 108114 (2020).
[18] K. Khishchenko, V. Fortov, and I. Lomonosov, Int. J. Thermophys. **26**, 479 (2005).
[19] V. L. Deringer, G. Csányi, and D. M. Proserpio, Chem. Phys. Chem. **18**, 873 (2017).
[20] J. Lahiri, Y. Lin, P. Bozkurt, I. I. Oleynik, and M. Batzill, Nat. Nanotechnol. **5**, 326 (2010).
[21] A. R. Botello-Mèndez, X. Declerck, M. Terrones, H. Terrones, and J.-C. Charlier, Nanoscale **3**, 2868 (2011).
[22] P. Simonis, C. Goffaux, P. Thiry, L. Biro, P. Lambin, and V. Meunier, Surf. Sci. **511**, 319 (2002).

[23] See Supplemental Material at http://link.aps.org/supplemental/10.1103/PhysRevLett.126.165501 for a crystallography information file providing detailed structural information of defect structures investigated.
[24] P. Giannozzi, O. Andreussi, T. Brumme, O. Bunau, M. B. Nardelli, M. Calandra, R. Car, C. Cavazzoni, D. Ceresoli, M. Cococcioni *et al.*, J. Phys. Condens. Matter **29**, 465901 (2017).
[25] A. Stone and D. Wales, Chem. Phys. Lett. **128**, 501 (1986).
[26] G. Csányi, C. J. Pickard, B. D. Simons, and R. J. Needs, Phys. Rev. B **75**, 085432 (2007).
[27] X. Li, Q. Wang, and P. Jena, J. Phys. Chem. Lett. **8**, 3234 (2017).
[28] M. A. Sheindlin and V. N. Senchenko, Sov. Phys. Dokl. **33**, 142 (1988).